The Emission Properties of Integrated Organic Light Emitting Diodes With Organic Photo Sensor for Emotional Lighting Applications

Jeong, J. W.; Park, Y. W.; Park, T. H.; Choi, J. H.; Choi, H. J.; Song, E. H.; Lee, J. I.; Chu, H. Y.; Ju, B. K.;
Display and Nanosystem Laboratory, College of Engineering, Korea University, Seoul,

This paper appears in: Electron Device Letters, IEEE
Issue Date: March 2011
Volume: 32 Issue:3
On page(s): 348 - 350
ISSN: 0741-3106
Digital Object Identifier: 10.1109/LED.2010.2099099
Date of Publication: 20 1월 2011
Date of Current Version: 22 2월 2011
Sponsored by: IEEE Electron Devices Society

ABSTRACT

This letter reports on a study of the emission properties of organic light-emitting diodes (OLEDs) controlled by an organic photo sensor (OPS) based on poly-3-hexylthiophene (P3HT) and [6, 6]-phenyl- $hbox{C}_{61}$ butyric acid methyl ester for emotional lighting applications. The emission characteristics exhibit the changes in the current and luminance of an OLED as a function of time when different illumination levels are exposed to the OPS. The luminance of the OLED increases from 283.4 to 1134 $hbox{cd/m}^{2}$ when the OPS is exposed to different illumination levels from full dark to 500 $hbox{mW/cm}^{2}$ using a xenon lamp.

The Emission Properties of Integrated Organic Light Emitting Diodes With Organic Photo Sensor for Emotional Lighting Applications

Jin Wook Jeong, Young Wook Park, Tae Hyun Park, Jin Hwan Choi, Hyun Ju Choi, Eun Ho Song, Jeong Ik Lee, Hye Yong Chu, and Byeong Kwon Ju, *Member, IEEE*

***Abstract*—This letter reports on a study of the emission properties of organic light-emitting diodes (OLEDs) controlled by an organic photo sensor (OPS) based on poly-3-hexylthiophene (P3HT) and [6, 6]-phenyl-C_{61} butyric acid methyl ester for emotional lighting applications. The emission characteristics exhibit the changes in the current and luminance of an OLED as a function of time when different illumination levels are exposed to the OPS. The luminance of the OLED increases from 283.4 to 1134 cd/m^2 when the OPS is exposed to different illumination levels from full dark to 500 mW/cm^2 using a xenon lamp.**

***Index Terms*—Emotional lighting, energy recycling, light sensor, organic light-emitting diodes (OLEDs), photo sensor.**

I. Introduction

EMOTIONAL lighting has recently attracted a great deal of attention for application in emotional engineering, because bright light is capable of increasing the body's production of certain hormones that control our alertness. These hormones increase our mental alertness and have a positive influence on our mental state, improving our mood without causing stress. Bringing sunlight into a human place lets us feel a more natural environment as the color temperature of the lighting changes as time passes during the day, similar to the light of sunrise, daylight, and sunset. The emotional lighting done by changing lighting levels and color temperature increases the stimulating capacity of the environment. Good lighting design can enhance pleasant and attractive surroundings, all while influencing behavior in a positive way. Thus, organic light emitting diode (OLED) lighting has been introduced as a promising light source for emotional lighting applications [1]–[4]. Organic photo sensors (OPSs) can be used for changing the lighting levels and color temperature of the OLEDs used by emotional sensors [5]–[12]. To analyze the environment, conjugated polymers have been widely used in organic photodiodes and organic photovoltaic devices because of their many advantages, such as simplified fabrication, low-temperatures process, low cost, good flexibility, high quantum efficiencies, and high-absorption coefficients [13]–[15]. An integrated OLED with an OPS can be applied to high-contrast displays, as well as emotional lighting applications. Light reflection can seriously degrade the contrast of an OLED display under a strong lighting environment since, even in the OFF-state, the device will still exhibit some brightness due to ambient-light reflection. Photon energies under a strong lighting environment are generated, which may be recycled by placing a photovoltaic cell in the back or at the side of an OLED. Thus, such a feature of energy recycling may be of significance and could be used for portable/mobile electronics, for such devices typically have high-power-awareness characteristics.

We studied the emission properties of OLED lighting controlled by an OPS based on P3HT:PCBM for emotional lighting or for high-contrast display applications. In addition, we will show that device-integrated OLED lighting with OPS increases the contrast of an OLED display subjected to a strong lighting environment.

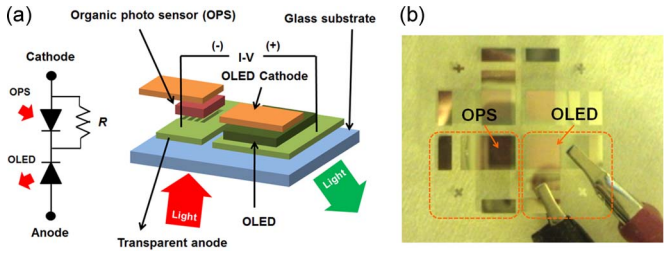

Fig. 1. (a) Schematic structure of the integrated OLED with OPS on the glass substrate. (b) Photographic image of the fabricated device.

II. Experiment

Fig. 1(a) shows the schematic structure for the integrated OLED with OPS on a glass substrate. The glass substrate with patterned indium thin oxide (ITO) film is used. The OPS for changing lighting levels and color temperature is fabricated by a solution process from blended P3HT:PCBM used as an electron donor and electron acceptor, respectively. The blend was prepared with P3HT:PCBM 1 : 0.8 ratio and dissolved in a 10-mg/ml solution with chlorobenzene. The P3HT:PCBM film was coated on the PEDOT:PSS coated ITO glass substrate using a spin-coating method. The thickness of the deposited

Manuscript received November 2, 2010; revised December 2, 2010; accepted December 4, 2010. Date of publication January 20, 2011; date of current version February 23, 2011. This work was supported in part by the IT R&D Program of MKE/KEIT under Grant 2009-F-016-01 (Development of Eco-Emotional OLED Flat-Panel Lighting), by the National Research Laboratory Program under Grant R0A-2007-000-20111-0, and by the World Class University Project of the Ministry of Education under Grant R32-2008-000-10082-0. The review of this letter was arranged by Editor P. K.-L. Yu.

J. W. Jeong, Y. W. Park, T. H. Park, J. H. Choi, H. J. Choi, E. H. Song, and B. K. Ju are with the Display and Nanosystem Laboratory, College of Engineering, Korea University, Seoul 136-713, Korea (e-mail: bkju@korea.ac.kr).

J. I. Lee and H. Y. Chu are with the Convergence Components and Materials Research Laboratory, Electronics and Telecommunications Research Institute, Daejeon 305-350, Korea.

Color versions of one or more of the figures in this letter are available online at http://ieeexplore.ieee.org.

Digital Object Identifier 10.1109/LED.2010.2099099

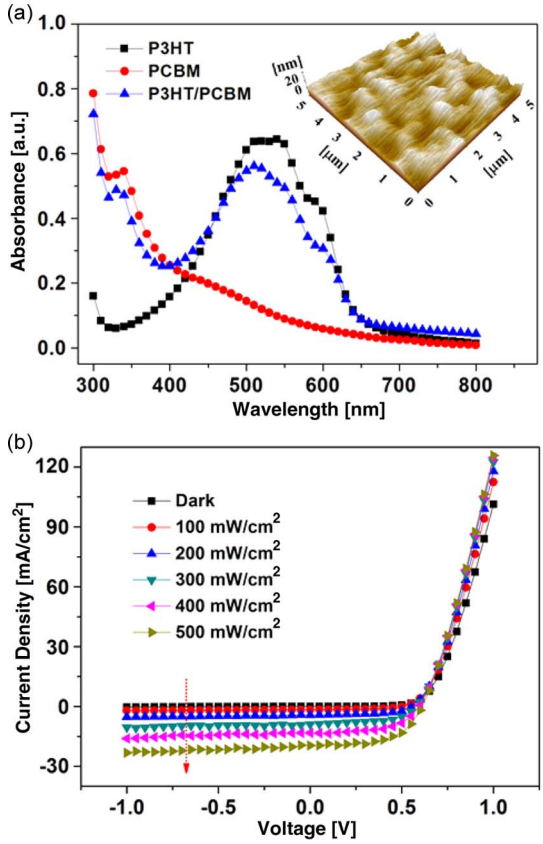

Fig. 2. (a) Measured absorption spectrum of pristine P3HT, pristine PCBM, and the blended P3HT:PCBM. Inset of (a) is the AFM image of the surface morphology of the OPS. (b) Current density versus voltage (I–V) characteristics of the OPS.

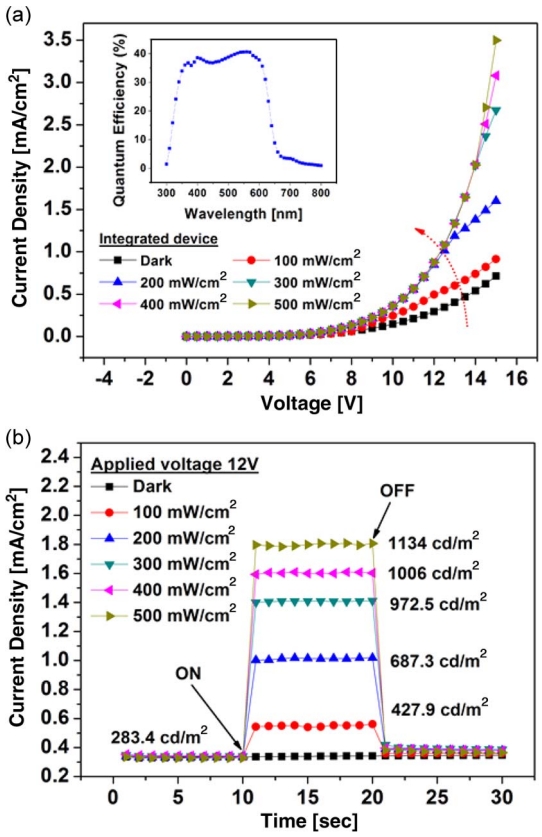

Fig. 3. (a) I–V characteristics of the integrated device. (b) Change in the current density as a function of time when exposed in the dark and under light intensities from 100 to 500 mW/cm^2 using a xenon lamp. Inset of (a) is the spectral dependence of the EQE of the OPS.

film was found to be about 170 nm. An aluminum electrode was deposited on the glass substrate by vacuum thermal evaporation using a shadow mask. The device was then annealed using a hot plate at 150 °C for 10 min. The OLED to be used for the lighting was fabricated to the side of the OPS, which had been patterned, and then cleaned by chemicals. The OLEDs are fabricated by the thermal evaporation of 40-nm n,n′-bis(naphtha-1-yl)-n,n′-bis(phenyl)-benzidine and 20-nm 4,4′,4″-tris(carbazol-9-yl)triphenylamine as the hole transporting layers; a 25-nm 4,4′-bis(carbazol-9-yl)biphenyl doped tris(2-phenylpyridine)iridium(III) (7%) is used for the emitting layer; a 10-nm 2, 9-dimethyl-4, 7-diphenyl-1,10-phenanhroline is used as the hole-blocking layer; a 45-nm 4, 7-Diphenyl-1, 10-phenanthroline is used as the electron transfer layer; and a 0.8-nm lithium fluoride and 100-nm aluminum are used as the cathode layer, consecutively. The fabricated integrated OLED with OPS is shown in Fig. 1(b).

III. Results and Discussion

Fig. 2(a) shows the measured absorption spectrum of each material: pristine P3HT, pristine PCBM, and blended P3HT:PCBM. The absorption spectrum of the pristine P3HT shows features of strong absorption in the visible spectrum, with an absorbance peak at 530 nm and two small shoulders at ∼550 and ∼600 nm. The pristine PCBM film shows a typical absorption peak at 340 nm, whereas the spectrum of the blended P3HT:PCBM shows one broad peak at 510 nm, as a contribution of the polymer, and one at 330 nm due to the absorption of the PCBM. With respect to the pristine P3HT, the absorption peak of the blended device is blue-shifted, and the whole spectrum is less structured due to the presence of the PCBM, which strongly limits the self-organizing property of the P3HT. However, blending the P3HT and the PCBM has been found to cover a wider visible spectral range. The inset image of Fig. 2(a) shows the atomic force microscopy (AFM) image of the surface morphology of the OPS annealed by hot plate in air. The root-mean-square roughness is 2.45 nm. The surface of the spin-coated organic film is both homogeneous and smooth. Fig. 2(b) shows the I–V characteristics of the OPS in the dark and under light intensities ranging from 100 to 500 mW/cm using a xenon lamp. The measured current density for the OPS is more rapidly achieved under a higher illumination level. It can be clearly observed that the current of the OPS increases due to an increase in the light illumination. The photovoltaic parameters of the OPS, such as the fill factor FF and efficiency $E_{\rm ff}$, can be calculated from the graph curve of Fig. 2(b). The OPS has a short-circuit current $J_{\rm sc}$ of 10.88 mA/cm^2 and an open-circuit voltage $V_{\rm oc}$ of 500 mV under an illumination level of 100 mW/cm^2.

Fig. 3(a) shows the I–V characteristics of the integrated device when exposed in the dark and under the light intensity from 100 to 500 mW/cm^2. The turn-on voltage and current density of the OLED lighting are 6.5 V and 0.04 mA/cm^2,

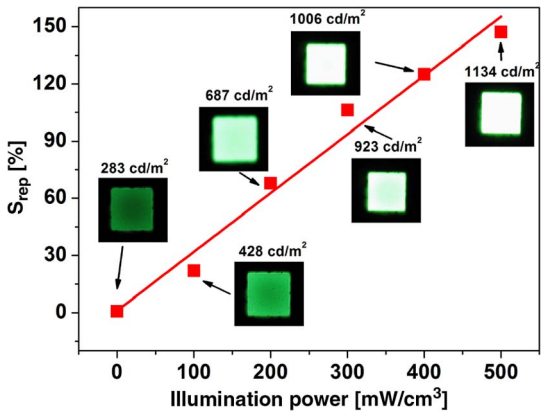

Fig. 4. Illumination versus power-luminance characteristics of the integrated OPS with OLED lighting.

respectively, under dark illumination power. As shown in the schematic structure of Fig. 1(a), the circuit of integrated device was formed in opposite directions. When the applied voltage between anode to cathode is fixed, the current flow from anode to cathode is largely dependent on OPS, because the series resistance of OPS is a dominant factor in deciding the total series resistance. The integrated device increased the operating voltage because of internal resistance R of OPS. In the I–V curve of the integrated device, the turn-on voltage decreased gradually when exposed to more illumination power, and the current density increased. Therefore, the generated dark current from the OPS under a strong lighting environment can be affected by changing lighting levels or the added self-powering function. In the inset of Fig. 3(a), the external quantum efficiency (EQE) of the OPS is shown to have a peak quantum efficiency of $\sim$40% around 350–600 nm. Fig. 3(b) shows the change in the current density as a function of time when the integrated device is exposed to the dark and under the light intensities from 100 to 500 mW/cm^2 using a xenon lamp, performed at room temperature in the atmosphere. The time dependence of the current density for the integrated device was measured at an applied voltage of 12 V. The luminance of the OLED increased from 283.4 to 1134 cd/m^2 when exposed under light intensities from dark to 500 mW/cm^2. Thus, it can be clearly observed that the OLED luminance increases due to an increase in the current density from the illumination power. Typical photodiodes should be used in the additional circuit because of the current levels of approximately nanoamperes under illumination power. However, the device of integrated OLED with OPS only changed the OLED luminance from the self-generated reverse current of OPS without the need for any additional circuit. In this letter, the self-generated reverse current from the OPS may be relatively small because the OPS and OLED devices were fabricated to the same size. However, by increasing the area of the OPS, the magnitude of this self-generated reverse current can be increased.

The sensitivity $S_{\rm rep}$ characteristics of the OPS are shown in Fig. 4, after being calculated from the graph curve of Fig. 3(b). The relative current change $S_{\rm rep} = (\Delta I_{\rm light}/I_{\rm dark}) \times 100$ is plotted against time for each illumination power level, with $I_{\rm dark}$ being the current baseline before exposure to the illumination power. The electrical effect of the OPS increases the luminance for the advanced current density of the OLED because of the dark current of the OPS under strong ambient illumination. The present recycling efficiency appears modest, yet it should be noted that the integrated OLED with OPS is simply for demonstration purposes; there is plenty of room for further raising of the recycling efficiency via more efficient OLED lighting and OPS structures, such as similar solar cells.

IV. Conclusion

This letter has reported on a study of the emission properties of OLED lighting controlled by an OPS based on P3HT and PCBM for emotional lighting or high-contrast display applications. The luminance of the OLED lighting increased from 283.4 to 1134 cd/m^2 when the integrated device was exposed to different illumination levels under a xenon lamp. As a result, the operation of the OLED lighting using series-interconnected OPSs could be successfully obtained. In addition, with power recycling, the devices themselves would have an added self-powering function and a higher system-level power efficiency.

References

[1] S. Reineke, F. Lindner, G. Schwartz, N. Seidler, K. Walzer, B. Lussem, and K. Leo, "White organic light-emitting diodes with fluorescent tube efficiency," *Nature*, vol. 459, no. 7244, pp. 234–238, May 2009.

[2] G. Schwartz, S. Reineke, T. C. Rosenow, K. Walzer, and K. Leo, "Triplet harvesting in hybrid white organic light-emitting diodes," *Adv. Funct. Mater.*, vol. 19, no. 9, pp. 1319–1333, May 2009.

[3] V. Bulovic, V. B. Khalfin, G. Gu, P. E. Burrows, D. Z. Garbuzov, and S. R. Forrest, "Weak microcavity effects in organic light-emitting devices," *Phys. Rev. B*, vol. 58, no. 7, pp. 3730–3740, Aug. 1998.

[4] Y. Sun, N. C. Giebink, H. Kanno, B. Ma, M. E. Thompson, and S. R. Forrest, "Management of singlet and triplet excitons for efficient white organic light emitting devices," *Nature*, vol. 440, no. 7086, pp. 908–912, Apr. 2006.

[5] X. Wang, O. Hofmann, R. Das, E. M. Barrett, A. J. deMello, J. C. deMello, and D. C. Bradley, "Integrated thin-film polymer/fullerene photodetectors for on-chip microfluidic chemiluminescence detection," *Lab Chip.*, vol. 7, no. 1, pp. 58–63, Jan. 2007.

[6] S. Tedde, E. S. Zaus, J. Furst, D. Henseler, and P. Lugli, "Active pixel concept combined with organic photodiode for imaging devices," *IEEE Electron Device Lett.*, vol. 28, no. 10, pp. 893–895, Oct. 2007.

[7] T. N. Ng, W. S. Wong, M. L. Chabinyc, S. Sambandan, and R. A. Street, "Flexible image sensor array with bulk heterojunction organic photodiode," *Appl. Phys. Lett.*, vol. 92, no. 21, pp. 213 303-1–213 303-3, May 2008.

[8] W.-Y. Wong, "Challenges in organometallic research—Great opportunity for solar cells and OLEDs," *J. Organometallic Chem.*, vol. 694, no. 17, pp. 2644–2647, Aug. 2009.

[9] P. Pistor, V. Chu, D. M. F. Prazeres, and J. P. Conde, "pH sensitive photoconductor based on poly(para-phenylene-vinylene)," *Sens. Actuators B, Chem.*, vol. 123, no. 1, pp. 153–157, Apr. 2007.

[10] A. El Amrani, B. Lucas, and A. Moliton, "Device based on the coupling of an organic light-emitting diode with a photoconductive material," *Thin Solid Films*, vol. 516, no. 7, pp. 1626–1628, Feb. 2008.

[11] E. Kraker, A. Haase, G. Jakopic, J. R. Krenn, S. Köstler, C. Konrad, S. Heusing, P. W. Oliveira, and M. Veith, "Organic photodiodes on flexible substrates," *Thin Solid Films*, vol. 518, no. 4, pp. 1214–1217, Dec. 2009.

[12] C.-J. Yang, T.-Y. Cho, C.-L. Lin, and C.-C. Wu, "Organic light-emitting devices integrated with solar cells: High contrast and energy recycling," *Appl. Phys. Lett.*, vol. 90, no. 17, pp. 173 507-1–173 507-3, Apr. 2007.

[13] S. H. Park, A. Roy, S. Beaupre, S. Cho, N. Coates, J. S. Moon, D. Moses, M. Leclerc, K. Lee, and A. H. Heeger, "Bulk heterojunction solar cells with internal quantum efficiency approaching 100%," *Nature Photon.*, vol. 3, no. 5, pp. 297–302, May 2009.

[14] S. F. Tedde, J. Kern, T. Sterzl, J. Furst, P. Lugli, and O. Hayden, "Fully spray coated organic photodiodes," *Nano Lett.*, vol. 9, no. 3, pp. 980–983, Mar. 2009.

[15] J. Y. Lee, S. T. Connor, Y. Cui, and P. Peumans, "Solution-processed metal nanowire mesh transparent electrodes," *Nano Lett.*, vol. 8, no. 2, pp. 689–692, Jan. 2008.